ELSEVIER

Journal of Nuclear Materials 279 (2000) 356–359

journal of nuclear materials

www.elsevier.nl/locate/jnucmat

Letter to the Editors

Densification behavior of U_3O_8 powder compacts by dilatometry

Kun Woo Song *, Keon Sik Kim, Youn Ho Jung

Advanced LWR Fuel Development, Korea Atomic Energy Research Institute, P.O. Box 105, Yusong, Taejon 305-600, South Korea

Received 4 November 1999; accepted 2 February 2000

Abstract

The densification behavior of U_3O_8 powder compacts has been investigated in a reducing atmosphere by dilatometry. The U_3O_8 compact shrank due to the reduction of U_3O_8 to UO_2 and then densified above 1200°C. The U_3O_8 compact containing simulated fission products densified more than the U_3O_8 compact. The addition of Nb_2O_5 enhanced significantly the densification rates of both compacts over the temperature range between 1200°C and 1600°C.

1. Introduction

Uranium dioxide (UO_2) fuel pellets have been widely used as a nuclear fuel. While UO_2 pellets are irradiated in a nuclear reactor, fissile materials are depleted and simultaneously fission products are produced. Spent fuel pellets, which have been irradiated to the design burnup, still include fissile materials that are worthwhile to be recycled. Thus, researches have been undertaken to fabricate new fuel pellets using spent fuel pellets.

According to the literature [1,2], irradiated UO_2 fuel pellets can be processed using a dry method to fabricate UO_2-based fuel pellets for reuse in a light water reactor. This cycle, the so-called AIROX cycle, includes the processes of producing U_3O_8-based powder by the oxidation of spent UO_2 fuel pellets and of producing sinterable UO_2-based powder from the U_3O_8-based powder. The terms 'UO_2-based' and 'U_3O_8-based' represent 'UO_2 containing fission products' and 'U_3O_8 containing fission products', respectively. Recently, the so-called DUPIC cycle [3] has been investigated for the purpose of processing irradiated UO_2 pellets and refabricating UO_2-based fuel pellets for reuse in a CANDU reactor.

It has been known [1,2] that the U_3O_8-based powder has to be further treated (oxidized and reduced) several times to have a suitable sinterability since it is not capable of making a pellet with a proper density. Process control associated with such powder treatments is difficult and time-consuming, for they have to be conducted remotely in a shielded cell. Therefore, it is necessary to refabricate fuel pellets using the U_3O_8-based powder without powder treatments.

The authors recently found that the powder mixture consisting of UO_2 and U_3O_8 powders, which had intrinsically a very low sinterability, could be sintered up to a high density by adding Nb_2O_5 or TiO_2 as a sintering additive [4,5]. The U_3O_8-based powder is supposed to be similar in physical properties to the U_3O_8 powder, so it is expected that such sintering additives could enhance densification in sintering the U_3O_8-based powder.

The purpose of this work is to study the densification behavior of U_3O_8 and U_3O_8-based powder compacts. The simulated UO_2 pellet, which can replicate a spent UO_2 fuel pellet, is made and then processed to make a U_3O_8-based compact. In addition, the effect of Nb_2O_5 addition on the densification behavior is investigated.

2. Experimental

UO_2 pellets, which had a density of 95.5% the theoretical density of UO_2 (10.96 g/cm^3) and a grain diameter

* Corresponding author. Tel.: +82-42 868 2579; fax: +82-42 868 2403.

E-mail address: kwsong@kaeri.re.kr (K.W. Song).

0022-3115/00/$ - see front matter
PII: S0022-3115(00)00025-8

of 7 μm, were oxidized at 400°C for 3 h in flowing air. During the oxidation a UO_2 pellet was spontaneously pulverized to U_3O_8 powder by the stress generated. The average particle size of U_3O_8 powder measured by a laser scattering method was 8 μm and the BET surface area of the powder was 0.5 m^2/g.

A special UO_2 fuel pellet was prepared to simulate a UO_2 pellet irradiated to 35 000 MWD/MTU in a light water reactor. The composition of an irradiated UO_2 pellet was calculated with the ORIGEN computer code [6] and of all the elements included in the irradiated UO_2 fuel pellet, 12 major chemical elements were selected. The powder mixture whose composition is shown in Table 1 was prepared using UO_2 powder and 12 non-radioactive chemical species. The powder mixture was ball-milled and granulated. Granules were pressed into compacts and sintered at 1650°C under H_2 gas to produce a simulated UO_2 fuel pellet. The simulated UO_2 fuel pellet had a density of about 96% the theoretical density, which was assumed to be 10.73 g/cm^3, and it had a grain diameter of about 6 μm.

It is expected that the composition of a simulated UO_2 pellet was slightly different from the powder composition in Table 1, since some changes occurred during sintering. $BaCO_3$ decomposed into BaO and CO_2 and the oxides in Table 1 were dissolved in UO_2 or formed precipitates, with some oxides such as CeO_2 and MoO_3 reduced.

Simulated UO_2 fuel pellets were oxidized at 450°C for 3 h in flowing air to produce U_3O_8-based powder, which was similar to the U_3O_8 powder in size and surface area. Nb_2O_5 was added in a quantity of 0.3 wt% to each of the U_3O_8 and U_3O_8-based powders. Four kinds of powders (U_3O_8 powders with and without Nb_2O_5, U_3O_8-based powders with and without Nb_2O_5) were pressed under 300 MPa into compacts. After a compact was set in a push rod type dilatometer, it was heated to 1650°C with 5°C/min under H_2 gas containing 1% H_2O by volume and then held for 4 h. The shrinkage of a compact was measured in an axial direction with a linear variable differential transformer (LVDT) transducer.

Table 1
Powder composition for the preparation of a simulated UO_2 pellet

Elements	Percentage by weight
SrO	9.147×10^{-2}
Y_2O_3	5.488×10^{-2}
ZrO_2	4.487×10^{-1}
MoO_3	4.737×10^{-1}
RuO_2	3.678×10^{-1}
Rh_2O_3	4.814×10^{-2}
PdO	1.464×10^{-1}
TeO_2	5.585×10^{-2}
$BaCO_3$	2.552×10^{-1}
La_2O_3	1.926×10^{-1}
CeO_2	9.186×10^{-1}
Nd_2O_3	6.605×10^{-1}
UO_2	96.286

3. Results and discussion

Fig. 1 shows the variations of length change ($\Delta L/L_0$) with temperature and holding time for the various compacts. The U_3O_8 compact undergoes a gradual expansion up to 500°C and a drastic shrinkage of about 8% between 500°C and 600°C. Le Page and Fane [7] found that the U_3O_8 phase was reduced to the UO_2 phase at temperatures of 500–600°C in hydrogen for less than 1 h. During the reduction the volume of U_3O_8 particle decreases theoretically by 23.6%, which is equivalent to about 7.9% in length, since the theoretical density increases from 8.37 to 10.96 g/cm^3. The drastic shrinkage of about 8% implies that the U_3O_8 compact shrinks during reduction nearly as a body of full U_3O_8.

The volume of U_3O_8 compact, however, is actually composed of both U_3O_8 particles and porosity and the U_3O_8 compact has a density of 5.59 g/cm^3 (66.8% in a fractional density). If only the volume of U_3O_8 particles shrinks due to the reduction, the compact can decrease only by 15.8% in volume, i.e., 5.3% in length. The drastic shrinkage is larger than 5.3%, so it can be deduced that the shrinkage of U_3O_8 compact includes not only the shrinkage of U_3O_8 particles but also the shrinkage of porosity. It is estimated that the porosity volume of U_3O_8 compact shrinks by the nearly same ratio as the volume of U_3O_8 particles. Consequently, the fractional density of U_3O_8 compact remains almost unchanged during the reduction of U_3O_8 to UO_2, in spite of the drastic shrinkage.

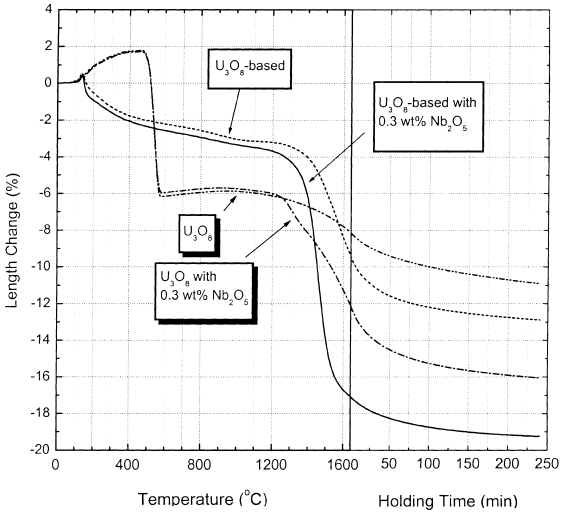

Fig. 1. Variations of shrinkage with temperature and holding time for U_3O_8 and U_3O_8-based compacts.

After the drastic shrinkage the compact appears not to shrink until about 1200°C and then it shrinks gradually to a final shrinkage of 11%. This final shrinkage originates from uranium reduction and densification and it is expected that only about 5% shrinkage of the 11% shrinkage is due to the densification of U_3O_8 compact.

The U_3O_8-based compact undergoes a gradual shrinkage over the temperature range 200–1200°C, and the related shrinkage is about 3%, which is much smaller than that of the U_3O_8 compact. This suggests that the shrinkage of U_3O_8-based compact does not include all the shrinkage of individual U_3O_8-based particles during reduction. Consequently, a considerable portion of the shrinkage of individual U_3O_8-based particles forms new porosity in a compact. It is supposed that the fractional density of U_3O_8-based compact decreases much due to the reduction, different from that of U_3O_8 compact. The U_3O_8-based compact begins to shrink at 1200°C and the final shrinkage of U_3O_8-based compact is about 13%. From the viewpoint of densification, it can be inferred that the U_3O_8-based compact undergoes some de-densification (decrease in compact density) below about 1200°C and densifies by about 10% shrinkage above 1200°C.

It can be readily seen that the addition of 0.3 wt% Nb_2O_5 has a very small effect on the shrinkage behavior of compacts below 1200°C but appears to enhance significantly the shrinkage above 1200°C. The U_3O_8 and U_3O_8-based compacts get the extra final shrinkage of about 5% and 6%, respectively, by adding 0.3 wt% Nb_2O_5. In other words, those compacts can be densified more effectively by the addition of 0.3 wt% Nb_2O_5.

Fig. 2 shows the variations of shrinkage rate ($\Delta L/L_0$/min) with temperature and holding time for the various compacts. It can be noticed that the shrinkage rates start to increase at about 1200°C for all the compacts. The shrinkage rate above 1200°C is supposed to be equivalent to the densification rate. As the temperature increases, the U_3O_8-based compact densifies with a higher rate than the U_3O_8 compact. The densification rate of U_3O_8-based compact has a remarkable maximum around 1550°C. It can be seen from Fig. 2 that the addition of Nb_2O_5 enhances significantly the densification rates of U_3O_8 and U_3O_8-based compacts in the temperature range 1200–1600°C, suggesting that the added Nb_2O_5 acts as a densification promoter in that temperature range.

The oxygen potentials ($RT \ln p(O_2)$) of niobium oxide and sintering gas were calculated using the HSC computer code [8] and the results are plotted in Fig. 3. A stable niobium oxide is dependent on temperature under hydrogen gas with 1% moisture; Nb_2O_5 below 820°C and NbO_2 between 820°C and 1650°C. Considering that the addition of Nb_2O_5 enhances significantly a densification rate in the temperature range 1200–1600°C, it is reasonable to suppose that NbO_2, a reduced product of Nb_2O_5, plays a dominant role in enhancing densification.

While the U_3O_8 compact with Nb_2O_5 is heated under the sintering gas, it is converted to a UO_2 compact with NbO_2 before the start of densification. If the Nb^{4+} ion enters interstitial site in the UO_2 structure during sintering, new uranium vacancies could be formed to maintain charge neutrality [4,9]. An increase in the concentration of uranium vacancy can enhance uranium diffusion, so it is expected that the densification of the UO_2 compact with NbO_2 progressed more rapidly.

As shown in Figs. 1 and 2, the U_3O_8-based compact exhibits a larger final densification and a higher densi-

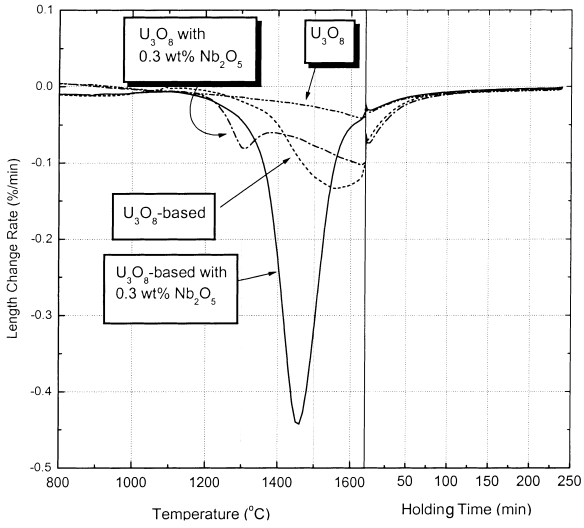

Fig. 2. Variations of shrinkage rate with temperature and holding time for U_3O_8 and U_3O_8-based compacts.

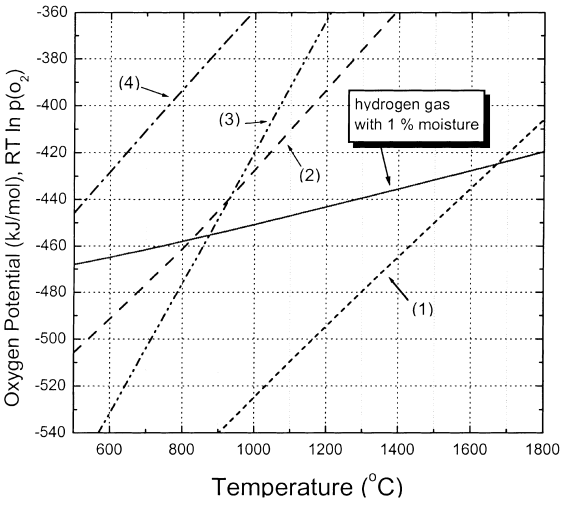

Fig. 3. Oxygen potentials of various oxides and sintering gas as a function of temperature. (1) $2NbO + O_2(g) = 2NbO_2$; (2) $4NbO_2 + O_2(g) = 2Nb_2O_5$; (3) $2Ce_2O_3 + O_2(g) = 4CeO_2(g)$; (4) $Mo + O_2(g) = MoO_2$.

fication rate than the U_3O_8 compact. This suggests that the addition of simulated fission products enhances the densification of U_3O_8 compact. Kleykamp [10] has reported that the fission products of irradiated fuel pellet are present in the form of dissolved oxides, metallic precipitates or oxide precipitates. It can be assumed that the chemical states of the simulated fission products are similar to those of real fission products. Of the simulated fission products in Table 1, MoO_3 and CeO_2 are present in considerable quantities and their chemical states are sensitively dependent on the oxygen potential, so their possible effects are primarily discussed. The Mo/MoO_2 and Ce_2O_3/CeO_2 equilibrium lines shown in Fig. 3 indicate that metallic Mo is stable in the whole temperature range and Ce_2O_3 is stable above about 900°C. The metallic Mo precipitate is likely to have an insignificant effect on the densification, but the dissolved Ce_2O_3 can change defect concentration in the UO_2 structure so that it could have some effect on the densification. It is supposed, however, that more experimental results are needed to discuss further the mechanisms by which the simulated fission products enhance densification.

While the U_3O_8-based compact with Nb_2O_5 is heated in the sintering gas, it is converted to a UO_2-based compact with NbO_2. During sintering the densification of this compact could be enhanced mainly by the same role of Nb^{4+} ion as the densification of the UO_2 compact with NbO_2 could be enhanced by. In addition, the simulated fission products might play some roles in the densification. It can be noticed from Fig. 1 that the U_3O_8-based and U_3O_8 compacts both gain a similar amount of additional densification by the addition of niobium oxide. This suggests that niobium oxide acts as a densification promoter even in the presence of the simulated fission products. Consequently, it would be reasonable to suppose that the simulated fission products do not obstruct the entrance of Nb^{4+} ion into the UO_2 structure.

4. Conclusions

As the compact of U_3O_8 powder is sintered in hydrogen, it drastically shrinks by 8% in length due to the reduction of U_3O_8 to UO_2 between 500°C and 600°C and then does not shrink further until 1200°C. The compact of U_3O_8-based powder shrinks gradually by about 3% over the temperature range between 200°C and 1200°C. It was estimated that the fractional density of U_3O_8 compact remained almost constant but that of U_3O_8-based compact decreased during the reduction. The U_3O_8 and U_3O_8-based compacts begin to densify at 1200°C and then the U_3O_8-based compact densifies with a higher rate than the U_3O_8 compact. Thus, the U_3O_8-based compact shows a greater final densification. The addition of Nb_2O_5 substantially enhances the densification rates of U_3O_8 and U_3O_8-based compacts over the temperature range between 1200°C and 1600°C and thus the compacts can densify by an additional 5–6% in length.

Acknowledgements

This work has been carried out under the Nuclear R&D Program supported by the Ministry of Science and Technology.

References

[1] S. Strausberg, NAA-SR-7138, 1962.
[2] J. Guon, J.E. Bodine, R.J. Sullivan, NAA-SR-8213, 1964.
[3] J.S. Lee, H.S. Park, R.D. Gadsby, J. Sullivan, Burn spent PWR fuel again in CANDU reactors by DUPIC, in: International Conference on Evaluation of Emerging Nuclear Fuel Cycle Systems, Versailles, France, September 1995, p. 355.
[4] K.W. Song, K.S. Kim, K.W. Kang, Y.H. Jung, J. Nucl. Mater. 207 (2000) 123.
[5] K.W. Song, K.S. Kim, K.W. Kang, Y.M. Kim, J. Korean, Nucl. Soc. 31 (1999) 455.
[6] M.J. Bell, ORIGEN-2 Code, ORNL-TM-4397, 1973.
[7] A.H. Le Page, A.G. Fane, J. Inorg. Nucl. Chem. 36 (1974) 87.
[8] HSC Chemistry for Windows, Outokump research, 1994.
[9] K.W. Song, K.S. Kim, K.W. Kang, Y.H. Jung, J. Korean, Nucl. Soc. 31 (1999) 335.
[10] H. Kleykamp, J. Nucl. Mater. 131 (1985) 221.